Eur Biophys J (1987) 14:349–358

European Biophysics Journal

Pore formation by Staphylococcus aureus alpha-toxin in lipid bilayers

Dependence upon temperature and toxin concentration

G. Belmonte, L. Cescatti, B. Ferrari, T. Nicolussi, M. Ropele, and G. Menestrina*

Dipartimento di Fisica, Universitá di Trento, I-38050 Povo (TN), Italy

Received June 9, 1986/Accepted in revised form September 30, 1986

Abstract. *Staphylococcus aureus* α-toxin forms ionic channels of large size in lipid bilayer membranes. We have developed two methods for studying the mechanism of pore formation. One is based on measurement of the ionic current flowing through a planar lipid membrane after exposure to the toxin; the other is based on measuring the release of the fluorescent complex Tb-Dipicolinic acid from large unilamellar vesicles under similar conditions.

Both methods indicate that the pore formation process is complex, showing an initial delay followed by non-linear kinetics. The power dependence of the pore formation rate on the toxin concentration in planar bilayers indicates that an aggregation mechanism underlies the channel assembly. Arrhenius plots, obtained with both techniques, show no deviation from linearity up to 50 °C and the derived activation energies are found to be comparable to those for the binding and the lysis of rabbit erythrocytes by the same toxin.

The temperature dependence of the conductance induced in planar bilayers by a large number of toxin channels indicates that the pores are filled with aqueous solution. The analysis of single conductance events shows that a heterogeneous population of pores exist and that smaller channels are preferred at low temperature. We attribute this heterogeneity to the existence of pores resulting from the aggregation of different numbers of monomers.

Key words: *Staphylococcus aureus,* α-toxin, ionic channel, activation energy, oligomerization, fluorescence, lipid vesicles, planar lipid membranes

* To whom offprint requests should be sent

Introduction

Staphylococcus aureus α-toxin is a cytolytic exotoxin which is secreted as a single water-soluble polypeptide with a molecular weight of 33,000 daltons (Freer and Arbuthnott 1983; Freer et al. 1973). The polypeptide is strongly surface active: it inserts into preformed lipid monolayers increasing their surface pressure (Freer et al. 1973; Bukelew and Colacicco 1971) and itself forms monolayers at an air-water interface (Bukelew and Colacicco 1971), suggesting that it can undergo a hydrophilic to amphiphilic transition. Also the protein has membrane-damaging properties and causes erythrocyte lysis via binding of the toxin to the cell membrane followed by ion leakage and finally hemoglobin release (Cassidy et al. 1974; Harshman 1979). The molecular events leading to membrane damage are not yet completely understood. On the basis of molecular weight analysis of protein extracts from lysed membranes it has been proposed that native α-toxin oligomerizes on the membrane to form an amphiphilic hexameric complex that, through its partial embeddment within the lipid bilayer, generates a transmembrane channel responsible for ion leakage (Füssle et al. 1981; Arbuthnott et al. 1973; Freer 1982). Attacked membranes do in fact show, under the electron microscope, characteristic lesions which appear as 10 nm diameter annular structures with 6-fold symmetry harbouring a 2–3 nm central pool of stain which may be related to the ion pathway (Freer and Arbuthnott 1983; Freer et al. 1973). A colloid-osmotic shock is thought to follow the leakage of ions, leading to the lysis of the membrane and ultimately to the death of the cell.

In order to investigate the mechanism of channel assembly and its relevance for the process of erythrocyte lysis we have studied the kinetics of pore formation on two biological model systems i.e. planar lipid bilayers and large unilamellar vesicles,

and its dependence on the toxin concentration and the temperature of the bath. We have found strong indications that the assembly of the pore is a multistep mechanism which involves several toxin monomers and that the activation energy for pore formation in model membranes is the same as that for the binding and lysis of rabbit erythrocytes by α-toxin (Cassidy and Harshman 1976; Ikigaj and Nakae 1984). This is good evidence that erythrocyte lysis is due to the formation of ionic channels in the lipid matrix of the cell.

Recently it has been shown that when α-toxin oligomerization is induced by deoxycholate smaller aggregates comprising 4 to 5 monomers can be formed together with the fully developed hexameric complex (Tobkes et al. 1985). Consistently, we have found that a heterogeneity in the population of channels can be explained by the existence of pores comprised of a different number of monomers.

Materials and methods

α-Toxin

Staphylococcus aureus α-toxin was a kind gift from Dr. K. D. Hungerer of the Behringwerke laboratories (Marburg, FRG). It has been shown by chromatography over Sephacryl S-300 that this preparation contains 75% of protein eluting in a sharp symmetrical peak of molecular weight 30 to 40 kDa corresponding to toxin monomers and 25% eluting in a second peak in the molecular weight region 180 to 500 kDa, corresponding to larger toxin aggregates (Bhakdi et al. 1981).

Planar bilayer experiments

Planar phospholipid bilayer membranes were prepared by the opposition of two monolayers with the Montal technique (Montal and Mueller 1972), using reduced egg phosphatidylcholine (PC, from P-L-Biochemicals, more than 99% pure). In some experiments stearoylmyristoylphosphorylcholine (SMPC, from Avanti Polar Lipids) was mixed with PC on a 1:1 basis. Monolayers were spread from a 5 mg/ml solution of these lipids in *n*-hexane and after evaporation of the solvent membranes were formed on a hole in a 12 μm thick Teflon septum separating two buffered salt solutions. The hole had a diameter of about 0.2 mm and was pretreated with a 1:20 solution of hexadecane in hexane. Bathing solutions, 4 ml on each side, contained various amounts of KCl, as specified in the text, 1 m*M* EDTA (Merck) and were buffered by 10 m*M* *Tris* (Calbiochem) at pH 7.0. The conductivity of each buffer solution has been measured with a Philips PW9509 digital conductimeter equipped with a PW9514 cell (cell constant 1 cm^{-1}). Unfractionated α-toxin from stock aqueous solution was added, after the membrane was completely formed and stabilized, to one compartment only (*cis* side) to a final concentration ranging from 5 to 250 μg/ml and the addition was followed by vigorous mixing of the solutions with magnetic bars. By means of two Ag-AgCl electrodes the transmembrane potential was clamped to the desired value and the current sent to an I−V converter built around a virtual grounded operational amplifier (Burr Brown OPA 104 C) with feed-back resistors ranging from 10^6 to 10^8 Ω. *Cis* compartment was connected to the virtual ground and voltage signs are referred to it; current is defined positive when cations flow into this compartment.

The temperature of the bathing solutions was controlled by means of an external circulator within ± 1 °C, and was measured directly by a digital thermometer (Keithley 871) with 0.1 °C accuracy.

Fluorescence experiments

Small unilamellar vesicles (SUV) were prepared as follows: 20 mg of PC, purified by an acetone extraction (Pick 1981) from egg lecithin (BDH) and dissolved in chloroform, were dried under a stream of nitrogen in a rotary evaporator (Büchi) and further connected to high vacuum for several hours. One milliliter of buffer containing 7.5 m*M* $TbCl_3$ (Riedel de Haen), 75 m*M* Sodium citrate, 75 m*M* Dipicolinic acid (DPA, from Sigma) and 2 m*M* *N-Tris*[hydroxymethyl]methyl-2-aminoethansulfonic acid (Tes, from Calbiochem), pH 7.0, was added and the solution mixed on a Vortex stirrer to obtain a milky liposome suspension. This was sonicated to clarity using a sonifier (Vibra Cell, from Sonics & Materials) equipped with a microtip (ca. 25 W output, 50% duty cycle, 20 min, room temperature). Large unilamellar vesicles (LUV) were then obtained by three successive cycles of freeze and thaw of this sonicate (Pick 1981), freezing was in liquid nitrogen, thawing at room temperature. Vesicles were separated from non-encapsulated material by gel filtration on Sephadex G-50 (Pharmacia) with an elution buffer consisting of 100 m*M* NaCl, 2 m*M* $CaCl_2$, 1 m*M* EDTA, 2 m*M* Tes, pH 7.0, and were used within the same day.

The release of the entrapped fluorescent complex, Tb-DPA, has been used to study the permeability effects induced by α-toxin. The release assay is based on the dissociation of the complex when it flows out from the vesicles into the external solution

where Tb^{3+} is chelated by EDTA resulting in a 10,000 fold decrease in the fluorescence intensity (Fraley et al. 1980; Bentz et al. 1983). We have chosen this experimental configuration in order to avoid the presence of free Tb^{3+} ions either inside the vesicles, where they are bound to DPA, or outside, where they are chelated by EDTA, since we have previously shown that free Tb^{3+} can close the α-toxin channels (Menestrina 1986). Fluorescence was measured with a Jasco FP 550 fluorimeter equipped with a thermostattable 4-cell sample turret. The temperature of the cuvette was controlled and measured as described for the planar bilayers. The Tb-DPA complex was excited at 276 nm and the emission was measured at 545 nm through an UV cut-off filter to eliminate any contribution from light scattering. A spontaneous leakage of the complex had a half-time of several hours and could be neglected in the analysis of our experiments in which α-toxin induced release was complete within one hour under the most unfavourable conditions.

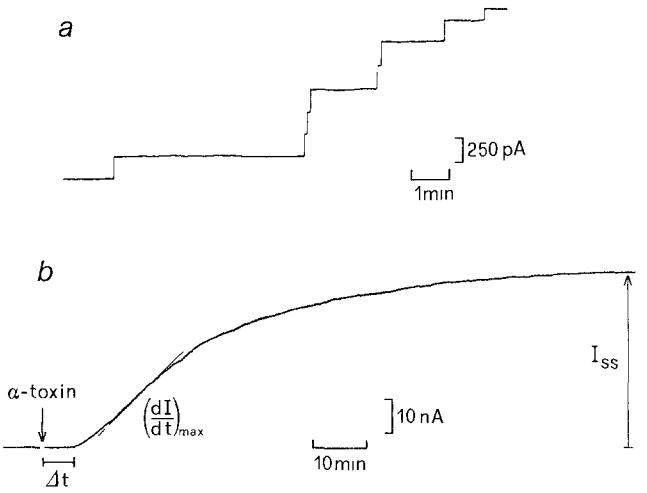

Fig. 1 a and b. Time course of the current flowing through a planar lipid bilayer after the addition of α-toxin to the bathing solution. **a** High current resolution. Discrete steps can be observed which each represent the opening of a new ionic channel. **b** Low current resolution. Current increases in an *s*-shaped way; it is possible to derive a delay time Δt, a maximum slope of the curve $(dI/dt)_{max}$ and a steady state value I_{ss}, as indicated on the figure. Experimental conditions are: KCl 0.5 *M*, pH 7.0; membranes consisting of PC; temperature 19 °C. Current and time scales are given in the figure, applied voltage was 40 mV

Results

Kinetic characterization of the interaction of α-toxin with lipid membranes

i. Planar lipid bilayers. Addition of *S. aureus* α-toxin on one side of a planar lipid bilayer causes the irreversible opening of ionic channels through the membrane (Menestrina 1986). Under voltage clamp conditions the formation of each channel can be resolved as a stepwise increase in the current flowing through the membrane, see for example Fig. 1 a. By averaging the heights of these steps we can calculate the mean conductance of the single channel produced by the toxin, which we call G_0. Alternatively, using low current resolution it is possible to follow the time course of the change in membrane conductance which is due to the insertion of a large number of channels into the lipid film. A typical trace is shown in Fig. 1 b: after the addition of the toxin the current flowing through the membrane increases in an *s*-shaped way i.e. after an initial time lag during which it remains at the bare membrane level, it starts increasing, it then reaches a maximum slope and it finally approaches a steady state value. It is possible to obtain an insight into the mechanism of channel formation from the kinetics of this process. To do this we have measured the lag time, Δt, (i.e. the time between the addition of the toxin and the formation of the first channel in the membrane), the maximum current slope $(dI/dt)_{max}$ and the final steady state current, I_{ss}, as a function of both the protein concentration and the temperature of the bath. Using the mean value of the single channel condutance, G_0, we obtain the maximum pore formation rate, μ_{max}, and the steady state number of pores in the membrane. N_{ss} as:

$$\mu_{max} = (dI/dt)_{max}/G_0 * V \quad (1)$$

$$N_{ss} = I_{ss}/G_0 * V, \quad (2)$$

where V is the constant voltage applied.

The dependence of $1/\Delta t$, μ_{max} and N_{ss} on the toxin concentration are shown in Fig. 2 a on a double logarithmic scale. Figure 2 b shows an Arrhenius plot of $1/\Delta t$ and μ_{max}; N_{ss} turned out to be almost independent of temperature ($N_{ss} = 600 \pm 250$).

ii. Lipid vesicles. As an alternative approach to the characterization of the kinetics of interaction of α-toxin with lipid bilayers we have studied its effects on LUVs loaded with the fluorescent complex Tb-DPA. The time course of the fluorescence of the vesicles after the addition of α-toxin is shown in Fig. 3 a for a typical experiment. After an initial time lag the fluorescence intensity decreases, indicating loss of the complex from the vesicles into the external solution. The approach to the steady state after the initial time lag, δt, can be described as the sum of two purely exponential components with different time constants, see Fig. 3 b. We call the two time constants τ_s and τ_f, referring to the slow and

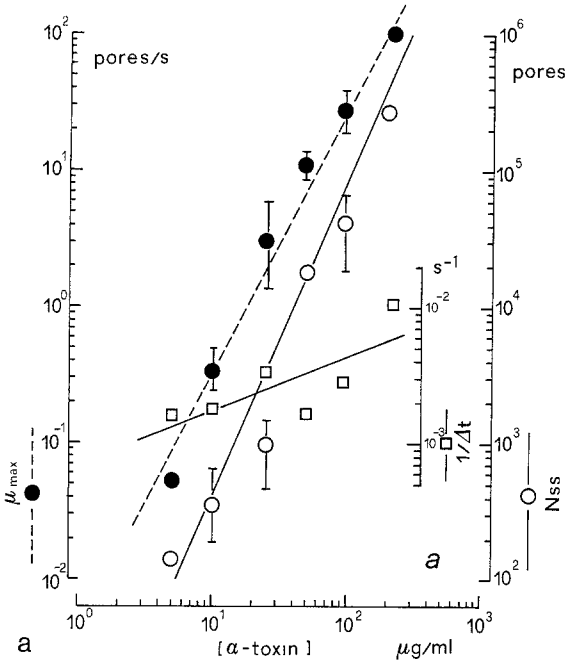

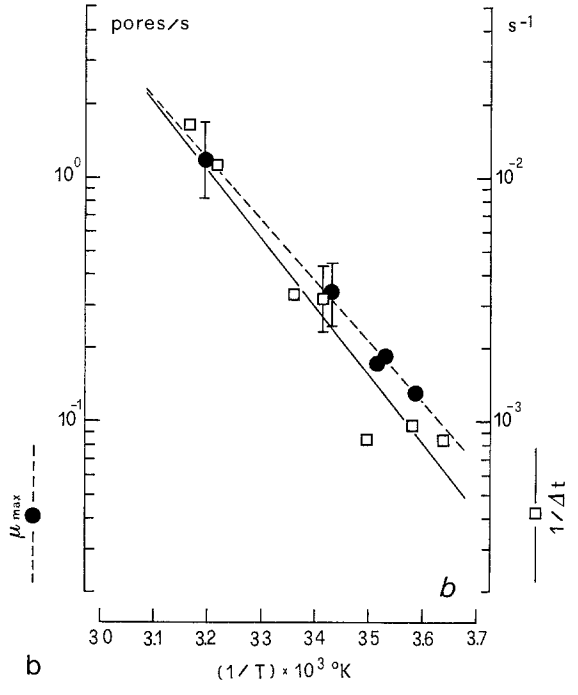

Fig. 2 a and b. Dependence of the pore formation parameters upon α-toxin concentration and bath temperature in planar lipid membranes. **a** Double logarithmic plot of the maximum pore formation rate, μ_{max}, the steady state number of channels, N_{ss}, and the reciprocal of the lag time, Δt, versus the toxin concentration. The slopes of the least squares lines are $n = 2.0$, 2.3 and 0.4 respectively. Bath temperature was 19 °C. **b** Arrhenius plot of μ_{max} and $1/\Delta t$. Activation energies are 11.3 and 12.7 kcal/mol respectively. α-toxin concentration was 50 μg/ml. Bathing solution was KCl 0.1 *M* in **a** and 0.5 *M* in **b**, pH 7.0. Other conditions as in Fig. 1

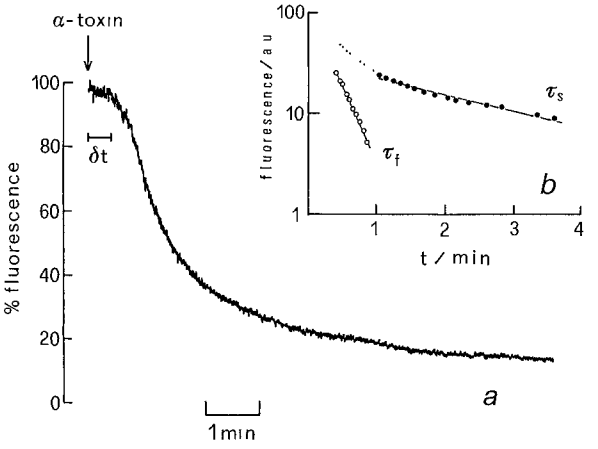

Fig. 3 a and b. Time course of the fluorescence of Tb-DPA loaded vesicles after the addition of α-toxin to the external solution. **a** Fluorescence decreases in an *s*-shaped fashion, it is possible to derive a lag time, δt, as indicated in the figure. **b** Semi-logarithmic plot of the digitized fluorescence in arbitrary units versus the time elapsed from the addition of the toxin, same trace as in **a**. The last part of the trace can be fitted with an exponential of time constant τ_s, full points. The first part of the trace, after the time δt, can be described with a single exponential with time constant τ_f once the slow component has been subtracted, open symbols. *Experimental conditions:* the composition of the external and internal solutions are given under materials and methods, pH 7.0; bath temperature 14.7 °C; α-toxin concentration 390 μg/ml

fast components respectively. The inital delay δt and both the time constants depend on the toxin concentration as well as on the temperature of the solution.

In Fig. 4a we show the reciprocals of the two time constants and of the time lag as a function of the toxin concentration in a double logarithmic plot, whereas in Fig. 4b the same quantities are reported as an Arrhenius plot to give the activation energies of the processes.

Temperature dependence of the α-toxin channel conductance

Additional information about the nature of the lesion produced by α-toxin in lipid bilayers can be obtained by studying the temperature dependence of the ionic conductance it induces in planar membranes.

An Arrhenius plot of the conductance through membranes containing a large and fixed number of α-toxin channels, which we call G_m, is shown in Fig. 5 and compared to the same plot for the conductivity of the bathing solution, σ. Membrane conductance was measured by varying the temperature of the bath after the incorporation of channels had been completed at a fixed temperature. In view of the fact that the pore formation rate, μ, is strongly

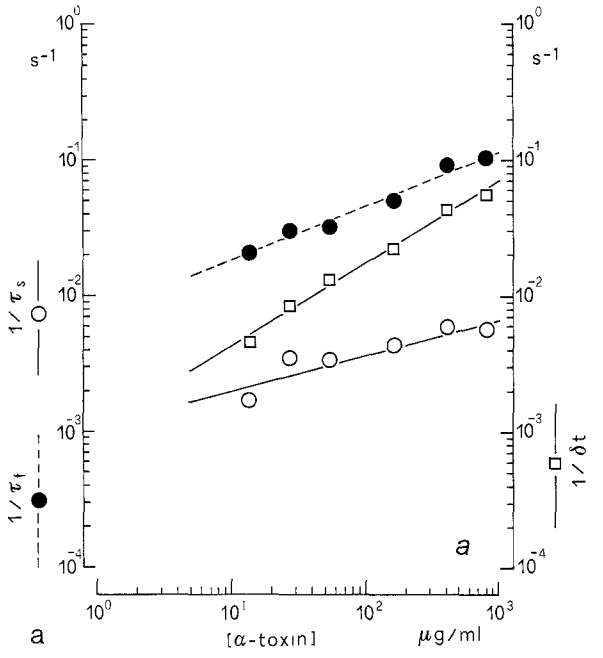

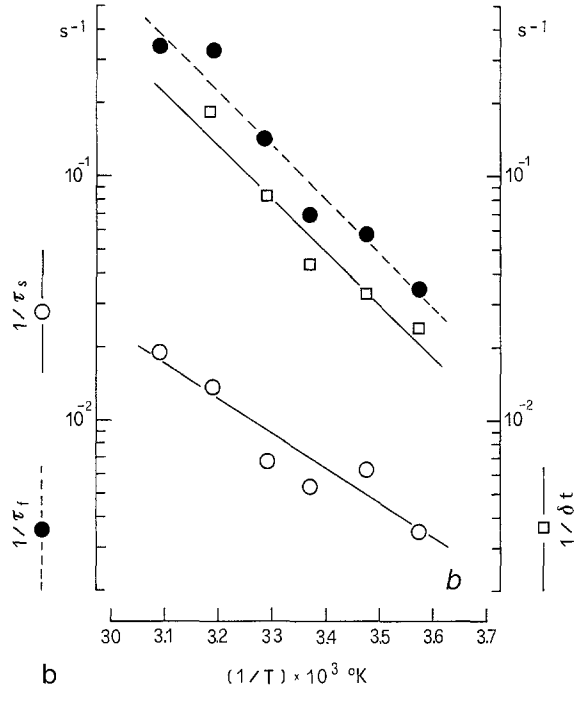

Fig. 4 a and b. Dependence of the pore formation parameters upon α-toxin concentration and bath temperature in lipid vesicles. **a** Double logarithmic plot of the reciprocal of the two time constants, τ_s and τ_f, and of the lag time, δt, versus the α-toxin concentration. The slopes of the least squares lines are $n = 0.25 \pm 0.10$, 0.40 ± 0.15 and 0.60 ± 0.16 respectively. Bath temperature was 23.3 °C. **b** Arrhenius plots of the reciprocal of the two time constants τ_s and τ_f and of the delay, δt. Activation energies are 6.4 ± 2.2, 10.1 ± 4.0 and 9.9 ± 2.0 kcal/mol respectively. α-toxin concentration was 390 μg/ml. Other experimental conditions as in Fig. 3

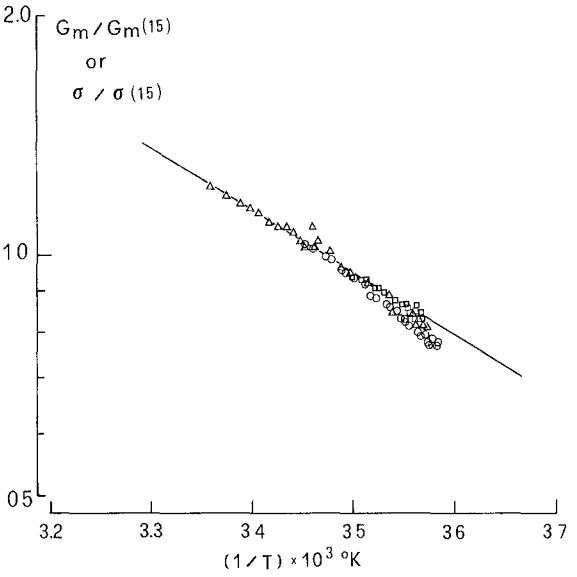

Fig. 5. Temperature dependence of the current flowing through a planar lipid membrane containing many α-toxin channels. Results from three different experiments have been presented using different symbols. Solid line is the temperature dependence of the solution conductivity as measured with a conductimeter. Both membrane conductance, G_m, and solution conductivity, σ, have been normalized by dividing by their values at 15 °C. Activation energies are 3.4, 3.3 and 4.9 kcal/mol for the three different membranes and 3.4 kcal/mol for the solution. Experimental conditions as in Fig. 2b

temperature-dependent (see Fig. 2b) it was important to be sure that no we channels appeared during the experiment and therefore that all changes in the membrane conductance could be attributed to a variation in channel conductance and not to a variation in the number of channels. To do this, besides waiting for the steady state conductance to be reached before starting to change the temperature of the bath, we performed a consecutive cooling and heating of the membrane and used data only from those experiments in which the conductance during heating was the same as during cooling at a corresponding temperature, indicating that the number of channels had remained constant. For a direct comparison in Fig. 5, data from different membranes and from the solution conductivity have been normalized by dividing by their respective values at 15 °C; it is apparent that within experimental resolution the temperature dependence of the α-toxin induced conductance is the same as that of the solution conductivity.

An alternative approach is to measure the mean single channel conductance, G_0, in experiments in which the incorporation of the first channels (which can be successfully used to calculate G_0, see Fig. 1), is performed at different bath temperatures. The results of this kind of experiment are shown in

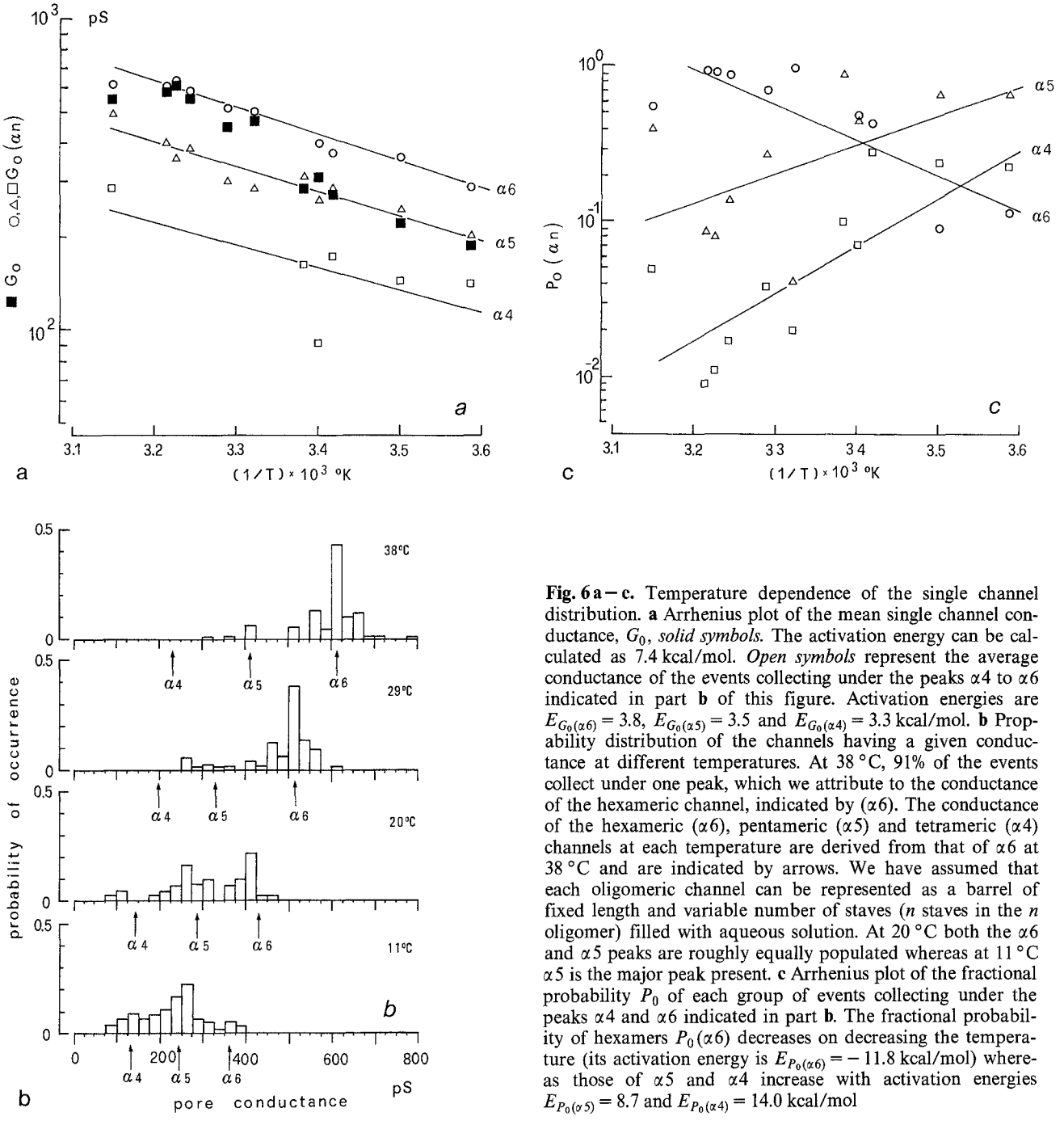

Fig. 6a–c. Temperature dependence of the single channel distribution. **a** Arrhenius plot of the mean single channel conductance, G_0, *solid symbols*. The activation energy can be calculated as 7.4 kcal/mol. *Open symbols* represent the average conductance of the events collecting under the peaks α4 to α6 indicated in part **b** of this figure. Activation energies are $E_{G_0(\alpha 6)} = 3.8$, $E_{G_0(\alpha 5)} = 3.5$ and $E_{G_0(\alpha 4)} = 3.3$ kcal/mol. **b** Probability distribution of the channels having a given conductance at different temperatures. At 38 °C, 91% of the events collect under one peak, which we attribute to the conductance of the hexameric channel, indicated by (α6). The conductance of the hexameric (α6), pentameric (α5) and tetrameric (α4) channels at each temperature are derived from that of α6 at 38 °C and are indicated by arrows. We have assumed that each oligomeric channel can be represented as a barrel of fixed length and variable number of staves (*n* staves in the *n* oligomer) filled with aqueous solution. At 20 °C both the α6 and α5 peaks are roughly equally populated whereas at 11 °C α5 is the major peak present. **c** Arrhenius plot of the fractional probability P_0 of each group of events collecting under the peaks α4 and α6 indicated in part **b**. The fractional probability of hexamers $P_0(\alpha 6)$ decreases on decreasing the temperature (its activation energy is $E_{P_0(\alpha 6)} = -11.8$ kcal/mol) whereas those of α5 and α4 increase with activation energies $E_{P_0(\alpha 5)} = 8.7$ and $E_{P_0(\alpha 4)} = 14.0$ kcal/mol

Fig. 6a, full points, in an Arrhenius plot. The temperature dependence now has a slope which is distinctly higher than that of the solution conductivity, as well as of the many channel conductance, G_m. As will be fully discussed later the reason for this apparent disagreement could be that the population of channels is heterogeneous. We have already shown (Menestrina 1986) that at room temperature the probability distribution of single channel conductances shows a major peak of high conductance but also an excess of events with lower conductance which have been attributed to smaller channels. We can show here, Fig. 6b, c that the probability distribution is also temperature-dependent, i.e. that at high temperatures only one major peak of high conductance can be seen, Fig. 6b upper panel, whereas at lower temperatures additional peaks of smaller conductance appear which broaden the whole probability distribution (Fig. 6b middle panels). We will show that the temperature dependence of the fractional probability of observing each of these peaks, Fig. 6c, provides the basis

to explain the different temperature dependence of G_m and G_0.

Discussion

Dependence of the kinetic parameters on α-toxin concentration

α-toxin is secreted by *S. aureus* as a 33 kDa water soluble polypeptide but it is now generally accepted that the lesion it produces on attacked cells is formed by a 200 kDa amphiphilic peptide resulting from the aggregation of six monomers (Füssle et al. 1981; Freer et al. 1973; Arbuthnott et al. 1973; Freer 1982). It is not yet clear whether the aggregation of the monomers occurs prior to their insertion into the bilayer or is the result of the interaction of pre-inserted monomers freely diffusing in the lipid bilayer.

We have found that the maximum pore formation rate, μ_{max}, and the maximum number of channels, N_{ss}, in a planar bilayer have a power dependence of 2.0 and 2.3 respectively, on the toxin concentration. These numbers, being relatively large, are a strong indication that an aggregation mechanism does indeed operate to produce the ionic channels. On the other side it is impossible to derive the true molecularity of the reaction from these exponents since μ_{max} is measured far from equilibrium and at least the last step in the formation of the hexamer has been found to be practically irreversible (Füssle et al. 1981).

In the framework of an aggregation mechanism of which only the last steps produce ionic channels into the lipid membrane, the lag time, Δt, would represent the time necessary for the first reaction steps to occur, which involve the formation of dimers and trimers. We have found for $1/\Delta t$ a power dependence on the toxin concentration of 0.4 i.e. much less than that of μ_{max} and N_{ss}, confirming that a lower number of monomers are involved in this process. It is worthwhile here to make a comparison with the case of gramicidin, a well known pore former which produces ionic channels by dimerization of monomers preinserted into the lipid bilayer. The exact solution of the dimerization kinetics shows that, under conditions of low peptide concentration, the number of dimers in the bilayer increases exponentially with time with a time constant whose reciprocal depends on the square root of the peptide concentration (Bamberg and Läuger 1973). Hence our value of exponent for the power dependence of $1/\Delta t$ on the toxin concentration is actually consistent with the reversible formation of dimers as a step preceding the opening the channels. Fully developed lesions could then arise from the aggregation of these preexisting dimers.

The study of the interaction of the toxin with lipid vesicles could in principle give similar information but care should be taken in the comparison of these results with those obtained with planar bilayers, owing to the differences which are inherent in the two systems. The decrease in the fluorescence produced by the toxin in vesicles loaded with the complex Tb-DPA indicates that this fluorescent probe, which has a molecular weight of 660 D, is released into the external solution. This is not surprising at all since we have shown that the ionic channels produced by α-toxin have a large diameter, ca. 12 Å, sufficient to allow the passage of solutes of molecular weight up to 1−2 kDa, as also found by others (Füssle et al. 1981). The decrease in fluorescence is thus the consequence of the formation of α-toxin channels in the LUVs. On the other hand since the formation of just one ionic channel into a lipid vesicle, in view of its high conductance, is sufficient to release all of its internal content within one second, the rate of decrease of fluorescence does not represent the pore formation rate but rather the rate of disappearance of intact vesicles or the rate of formation of the very first ionic channel into each vesicle. As a result we expect only the power dependence of the lag time δt to be comparable to that of Δt in the planar bilayer system, since both these quantities deal with the events preceding the formation of the first ionic channel, and this is what we have indeed observed. The two time constants τ_s and τ_f give an estimate of the rate of disappearance of intact vesicles which is only a rough estimate of the pore formation rate; consequently their power dependence on the toxin concentration has an exponent which is much lower than the one corresponding to μ_{max} in planar bilayers. Nevertheless the fact that the kinetics of the process are not simple, i.e. it cannot be described by a single exponential component but needs the sum of a delay time plus two exponential components, is a strong indication that the reaction leading to the formation of ionic channels is a multistep one as expected for an aggregation mechanism.

Dependence of the kinetic parameters on the temperature

From the Arrhenius plots in Figs. 2b and 4b it is possible to calculate the activation energies of the events preceding the formation of ionic channels, plots of Δt and δt, and for the events leading to the opening of the pores, plots of μ_{max} and τ_s, τ_f. We have found: $E_{1/\Delta t} = 12.7 \pm 2.0$, $E_{1/\delta t} = 9.9 \pm 2.0$ and $E_{\mu_{max}} = 11.3 \pm 1.5$, $E_{1/\tau_s} = 6.4 \pm 2.0$, $E_{1/\tau_f} = 10.1 \pm 4.0$ kcal/mol. There is generally good agreement be-

tween the values obtained with the two different techniques; particularly the values of activation energy obtained for the two decay times are so large (roughly 3–4 times the energy of activation for the diffusion of a macromolecule in the aqueous solution; Nikaido and Rosenberg 1981) that one may exclude the possibility that they are due to the diffusion of the toxin through the water phase up to the plane of the membrane.

It is interesting to compare our values with the activation energies for the binding of α-toxin to rabbit erythrocytes (Cassidy and Harshman 1976) and their subsequent lyses (Ikigaj and Nakae 1984). From the linear part of these plots (i.e. for $0 < T < 30\,^{\circ}C$) it is possible to derive $E_{bind} = 9.0$ and $E_{lysis} = 11.4$ kcal/mol. Both these values are similar to those we have found for the pore formation mechanism (mean value $E = 10.1 \pm 1.2$ kcal/mol). The fact that the activation energies for the binding of α-toxin to erythrocytes, for their lysis and for the formation of ionic channels in lipid bilayers are the same suggests that a unique phenomenon is actually underlying these events. On the other hand one should notice that both the Arrhenius plots obtained with rabbit erythrocytes (Cassidy and Harshman 1976); Ikigaj and Nakae 1984) display a large deviation from linearity above approximately 30 °C, with a decrease in both binding and lysing efficiency of the toxin at higher temperatures. Since we have found no break in the Arrhenius plot up to 50 °C we can conclude that the non-linearity in that case was due to some peculiar component of the erythrocyte membrane other than the toxin and the phospholipid matrix.

Finally it is worth comparing the activation energies we have found (mean value $E = 10.1 \pm 1.2$ kcal/mol) with that for the microviscosity of an egg PC bilayer (Jain and Wagner 1980) which is $E_{\mu visc} = 7.3$ kcal/mol. In view of the similarity between the two values it is attractive to speculate that the diffusion in the plane of the membrane of toxin monomers or dimers, which would be primarily determined by the fluidity of the membrane, is the rate limiting step for the formation of ionic channels. This would fit nicely into an aggregation model and actually a similar value, 12 kcal/mol, has been found for the pore state lifetime of the alamethicin channel, a well known example of a channel resulting from the aggregation of monomers (Boheim and Kolb 1978).

Dependence of channel conductance on the temperature

The Arrhenius plot of Fig. 5 indicates that the activation energy for the transport of ions through a membrane containing many α-toxin channels is $E_{G_m} = 3.8$ kcal/mol. This is practically the same activation energy as for the conductivity of the ionic solution itself ($E = 3.9$ kcal/mol for a 1 *M* KCl (Harned and Owen 1958)). The obvious interpretation of this finding is that α-toxin channels are filled with water solution; this is fully consistent with out previous finding that the conductance of the channel varies linearly with that of the solution when the concentration of the electrolyte is changed (Menestrina 1986). Actually the diameter of the channel which can be estimated from the linear relationship between pore conductance and solution conductivity, i.e. 11.4 ± 1.0 Å (Menestrina 1986), is large enough to permit the passage of ions in a fully hydrated form. A similar result has also been found with other pore formers which produce ionic channels of high conductance, for example alamethicin (Boheim and Kolb 1978), porin (Nikaido and Rosenberg 1981) and EIM (Latorre et al. 1974) and in those cases also the result has been interpreted as indicating that the channels are filled with aqueous solution. When the mean single channel conductance, G_0, is reported in a similar Arrhenius plot (Fig. 6a full points) a larger activation energy is obtained: $E_{G_0} = 7.4$ kcal/mol. The reason for this apparent discrepancy is to be found in heterogeneity of the channel population. We have already noticed that the probability distribution of the single channel conductances is not homogeneous, showing an excess of smaller events in addition to a well defined major peak (Menestrina 1986). We have attributed these smaller events to the presence of channels consisting of only 5 monomers instead of 6, which have a smaller conductance owing to the smaller cross sectional area. This hypothesis is consistent with the results of a recent study on the aggregation behavior of this toxin induced by deoxycholate (Tobkes et al. 1985). SDS-polyacrylamide gel electrophoresis has shown the presence near the major band of molecular weight 200 kDa of two lighter bands which were thought to represent pentamers and tetramers. The three bands were named α6, α5 and α4, with the numbers representing the number of monomers comprising the aggregate. We will use the same nomenclature here. Even earlier electron microscopy studies revealed the presence of aggregates ranging from 5 to 7 monomers with the preference for hexamers (Freer et al. 1973).

It is conceivable that in planar lipid membranes smaller aggregates can form under conditions unfavorable for the formation of the complete hexamer, such as low toxin concentration or low temperature. It is also conceivable that even preaggregates like pentamers and tetramers could produce ionic channels through the lipid bilayer though with

a lower conductance, as is the case of the well known pores formed by aggregates of the antibiotic alamethicin or nystatin, which can consist of a different number of monomers (Boheim and Kolb 1978; Kleinberg and Finkelstein 1984). As in those cases we can assume that the ionic conductances of pores consisting of a different number of monomers are proportional to the cross sectional area of regular polygons with same side length but different number of sides (barrel stave model; Boheim and Kolb 1978).

Inspection of panel *A* of Fig. 6 b indicates that at high temperature only one major peak is present, which we assume to correspond to fully developed hexameric channels. If we call $G(\alpha 6)$ the conductance of the hexameric channel we can predict the conductance of pores consisting of 5 or 4 monomers, $G(\alpha 5)$ and $G(\alpha 4)$, at each temperature using the barrel stave model and the assumption that each type of pore is filled with water. The values of $G(\alpha 6)$, $G(\alpha 5)$ and $G(\alpha 4)$ are indicated by arrows on each panel of Fig. 6 b. It indeed appears that the probability distribution has peaks that correspond with these values and that the probability of observing smaller channels increases when the temperature is decreased. We have used the position of these arrows to calculate the mean conductance $G_0(\alpha n)$ $n=4$ to 6) and the fractional probability $P_0(\alpha n)$ of each group of events around an arrow. Experimental $G_0(\alpha n)$ are shown in Fig. 6 a, open symbols, and the corresponding activation energies are $E_{G_0(\alpha 6)} = 3.8$; $E_{G_0(\alpha 5)} = 3.5$ and $E_{G_0(\alpha 4)} = 3.3$ kcal/mol, i.e. the same as the conductivity of the solution within experimental error. Furthermore, at each temperature the ratios between the mean channel conductances $G_0(\alpha n)$ are 2.7 : 1.8 : 1 corresponding to $\alpha 6 : \alpha 5 : \alpha 4$ whereas those of the areas of the regular polygons are 2.6 : 1.7 : 1 in the same order. The values of $P_0(\alpha n)$ are reported in Fig. 6 c; it appears that $P_0(\alpha 6)$ decreases with temperature, while $P_0(\alpha 5)$ and $P_0(\alpha 4)$ increase in the same direction ($E_{P_0(\alpha 6)} = -11.8$, $E_{P_0(\alpha 5)} = 8.6$ and $E_{P_0(\alpha 4)} = 14.0$ kcal/mol).

As shown in the appendix this model is able to reconcile the apparent inconsistency between the values of E_{G_m} and E_{G_0}, since each channel type is actually full of water, as indicated by E_{G_m}, but the probability of observing different channels, depending itself on the temperature, produces the larger value of E_{G_0}.

The reason for the temperature dependence of the $P_0(\alpha n)$ seems to be found in the variation of the membrane fluidity. Decreasing the temperature in fact decreases the mobility of the non-conducting preaggregates (monomers and dimers) in the bilayer and hence the probability of formation of those aggregates which require a larger number of effective collisions to be formed. Consistent with this idea, we have found that the addition of 50% SMPC to the membrane (which owing to its high transition temperature, 30 °C (Chen and Sturtevant 1981), increases the bilayer viscosity) decreases the probability of the hexamer from $P_0(\alpha 6) = 0.92$ in PC membranes to $P_0(\alpha 6) = 0.78$ in PC/SMPC membranes at 37 °C and from 0.12 to 0.06 at 3 °C.

Appendix A

Let us assume that α-toxin channels can exist in different forms each consisting of a different number of monomers, 4 to 6, which we call $\alpha 4$ to $\alpha 6$, and that each type of pore has a conductance $G_0(\alpha n)$ and a fractional probability of occurrence $P_0(\alpha n)$, with $n=4$ to 6. Let us further assume that each channel, once formed, is stable and there is no further change in the number of monomers comprising it. This is actually reasonable since no change in the channel conductance can be seen after its formation and it has been shown that the formation of the hexameric aggregate is practically irreversible (it dissociates only when boiled in SDS; Freer and Arbuthnott 1983).

If all the channels are filled with aqueous solution we can write, for $n=4$ to 6:

$$G_0(\alpha n, T) = \frac{A_0(\alpha n)}{l} \sigma_0 \exp(-E_\sigma/kT) \tag{A1}$$

$$= g_0(\alpha n) \exp(-E_\sigma/kT), \tag{A2}$$

where $A_0(\alpha n)$ is the cross sectional area of the pore consisting of n monomers, l its length (assumed to be the same for all the species) and $\sigma_0 \exp(-E_\sigma/kT)$ is the conductivity of the solution. The applicability of this expression is confirmed by the experimental results shown in Fig. 6 a, open symbols.

In general we will have probabilities, $P_0(\alpha n)$, of the type:

$$P_0(\alpha n, T) = p_0(\alpha n) \exp(-E_{P_0(\alpha n)}/kT) \tag{A3}$$

as is demonstrated by Fig. 6 c.

The conductance, G_m, of a membrane containing N channels incorporated at a temperature T_0 is then given by:

$$G_m(T) = N \sum_{n=4}^{6} P_0(\alpha n, T_0)\, G_0(\alpha n, T) \tag{A4}$$

$$= N \sum_{n=4}^{6} p_0(\alpha n) \exp(-E_{P_0(\alpha n)}/kT_0)\, g_0(\alpha n) \cdot \exp(-E_\sigma/kT) \tag{A5}$$

$$= G_{m_0} \exp(-E_\sigma/kT) \tag{A6}$$

and hence its activation energy E_{G_m} is just that of the solution conductivity E_σ.

On the other hand the mean single channel conductance G_0 of a population of channels observed at a temperature T is:

$$G_0(T) = \sum_{n=4}^{6} P_0(\alpha n, T)\, G_0(\alpha n, T) \tag{A7}$$

$$= \sum_{n=4}^{6} p_0(\alpha n)\, g_0(\alpha n) \cdot \exp\left(-\left(E_{P_0(\alpha n)} + E_\sigma/kT\right)\right) \tag{A8}$$

and in this case we find that the activation energy for the single channel conductance, E_{G_0}, is different from that of the solution, E_σ.

References

Arbuthnott JP, Freer JH, Billcliffe B (1973) Lipid-induced polymerization of Staphylococcal α-toxin. J Gen Microbiol 75:309–319

Bamberg E, Läuger P (1973) Channel formation kinetics of gramicidin A in lipid bilayer membranes. J Membr Biol 11:177–194

Bentz J, Düzgünes N, Nir S (1983) Kinetics of divalent cation induced fusion of phosphatidylserine vesicles; correlation between fusogenic capacities and binding affinities. Biochemistry 22:3320–3330

Bhakdi S, Füssle R, Tranum-Jensen J (1981) Staphylococcal α-toxin: oligomerization of hydrophilic monomers to form amphiphilic hexamers induced through contact with deoxycholate detergent micelles. Proc Natl Acad Sci USA 78: 5475–5479

Boheim G, Kolb HA (1978) Analysis of the multi-pore system of alamethicin in a lipid membrane. I. Voltage-jump current-relaxation measurements. J Membr Biol 39:99–150

Bukelew AR, Colacicco G (1971) Lipid monolayers. Interaction with Staphylococcal α-toxin. Biochim Biophys Acta 233:7–16

Cassidy P, Six AR, Harshman S (1974) Biological properties of Staphylococcal α-toxin. Biochim Biophys Acta 332: 413–425

Cassidy P, Harshman S (1976) Studies on the binding of Staphylococcal ^{125}I-labelled α-toxin to rabbit erythrocytes. Biochemistry 15:2348–2355

Chen SC, Sturtevant JM (1981) Thermotropic behavior of bilayers formed from mixed-chain phosphatidylcholines. Biochemistry 20:713–718

Fraley R, Wilschut J, Düzgünes N, Smith C, Papahadjopoulos D (1980) Studies on the mechanism of membrane fusion: Role of phosphate in promoting calcium ion induced fusion of phospholipid vesicles. Biochemistry 19:6021–6029

Freer JH (1982) Cytolytic toxins and surface activity. Toxicon 20:217–221

Freer JH, Arbuthnott JP (1983) Toxins of Staphylococcus aureus. Pharmacol Ther 19:55–106

Freer JH, Arbuthnott JP, Bilcliffe B (1973) Effects of Staphylococcal α-toxin on the structure of erythrocytes membranes. J Gen Microbiol 75:321–332

Füssle R, Bhakdi S, Sziegoleit A, Tranum-Jensen J, Kranz T, Wellensiek HJ (1981) On the mechanism of membrane damage by Staphylococcus aureus α-toxin. J Cell Biol 91: 83–94

Harned S, Owen B (1958) The physical chemistry of electrolytic solutions. Reinhold, New York

Harshman S (1979) Action of staphylococcal α-toxin on membranes: some recent advances. Mol Cell Biochem 23: 142–152

Ikigai H, Nakae T (1984) The rate assay of alpha-toxin assembly in membrane FEMS. Microbiol Lett 24:319–322

Jain K, Wagner C (1980) Introduction to biological membranes. John Wiley and Sons, New York

Kleinberg ME, Finkelstein A (1984) Single-length and double-length channels formed by nystatin in lipid bilayer membranes. J Membr Biol 80:257–269

Latorre R, Alvarez O, Verdugo P (1974) Temperature characterization of the conductance of the excitability inducing material channel in oxidized cholesterol membranes. Biochim Biophys Acta 367:361–365

Menestrina G (1986) Ionic channels formed by Staphylococcus aureus alpha-toxin: voltage dependent inhibition by di and trivalent cations. J Membr Biol 90:177–190

Montal M, Mueller P (1972) Formation of bimolecular membranes from lipid monolayers and a study of their electrical properties. Proc Natl Acad Sci USA 69:3561–3566

Nikaido H, Rosenberg Y (1981) Effect of solute size on diffusion rates through the transmembrane pores of outer membrane of *Escherichia coli*. J Gen Physiol 77:121–135

Pick U (1981) Liposomes with a large trapping capacity prepared by freezing and thawing of sonicated phospholipid mixtures. Arch Biochem Biophys 212:186–194

Tobkes N, Wallace BA, Bayley H (1985) Secondary structure and assembly mechanism of an oligomeric channel protein. Biochemistry 24:1915–1920